Materials Characterization 139 (2018) 233–240

Contents lists available at ScienceDirect

Materials Characterization

journal homepage: www.elsevier.com/locate/matchar

Interfacial microstructure evolution and weld formation during ultrasonic welding of Al alloy to Cu

H.T. Fujii*, H. Endo, Y.S. Sato, H. Kokawa

Department of Materials Processing, Graduate School of Engineering, Tohoku University, 6-6-02 Aramaki-aza-Aoba, Aoba-ku, Sendai 980-8579, Japan

ARTICLE INFO

Keywords:
Aluminum alloy
Copper
Ultrasonic welding
Oxide layer
Intermetallic compound

ABSTRACT

Dissimilar welds of Al alloy 1050 to Cu were prepared via ultrasonic spot welding in order to understand the formation of welds and interfacial microstructures. To observe oxide layer behavior at the weld interface, the anodized Al alloy 1050 was also welded to Cu. Mechanical mixing and material flow during ultrasonic welding broke and dispersed the oxide layers into the Al matrix. This material flow is attributed to compressive deformation that occurred due to ultrasonic vibrations. Direct bonding in the Al/Cu region increased with welding time. Once micro-bonds were generated between Al and Cu, the Al matrix in the vicinity of the weld interface was severely deformed in the direction of the ultrasonic vibrations. Consequently, a recrystallized microstructure with shear texture was formed in the Al matrix. Deformation heating and severe shear deformation formed Al_2Cu intermetallic compound layers at the weld interface. The growth rate of the Al_2Cu layer was much faster than had previously been estimated based upon the peak temperature and ultrasonic welding heating time. This is likely due to the increased rate of Cu diffusion into Al in the severely deformed region.

1. Introduction

Ultrasonic vibrations can be used to join metals via interactions with many metallurgical phenomena [1–5]. Ultrasonic metal welding is a solid state welding technique that combines ultrasonic vibrations with a normal clamping force. This technique is characterized by its short welding time, low welding energy, small welding distortion, and lower environmental burden than other solid-state welding techniques [6–8]. Notably, ultrasonic metal welding allows thin metallic components such as metallic foils, wires, and plates to be welded much more easily than conventional welding techniques. Thus, ultrasonic metal welding exhibits promise for various manufacturing applications. Recently, attention has shifted to dissimilar welding between light metals and other metals for weight reduction in industrial products. In particular, development of techniques for welding Al alloys to Cu is needed to support the automotive and electrical industries because recent vehicles include a number of electrical components.

Thus far, several studies have characterized ultrasonic welds between Al alloys and Cu [9–22]. Zhao et al. observed voids, swirl-like structures, and intermetallic compound layers around weld interfaces after ultrasonic spot welding (USW) of Al alloy 6061 to pure Cu [12]. They concluded that the swirls led to mechanical interlocking between the materials, resulting in increased weld strength. Balasundaram et al. clarified the effects of zinc interlayers on USW of Al alloy 5754 to pure Cu [13]. Welds with a Zn interlayer formed an eutectic structure of Al and Al_2Cu intermetallic compounds around the interface, drastically improving their lap shear tensile strengths. Zhang et al. observed the fracture surfaces and cross-sections of weld interfaces via scanning electron microscopy (SEM) [16] after USW of Al ribbons to Cu sheets. They clarified the formation of secondary interfaces and interfacial void shrinkage mechanisms during USW. Ni et al. obtained sound welds of Al to Cu via USW with an Al alloy 2219 particle interlayer [18]. Because this particle interlayer was added, it is thought that deformation heating promoted weld formation during USW. In addition, the weld behaviors of each layer in multiple-layered Al—Cu samples fabricated via USW were studied by Shin et al. for applications in lithium ion battery manufacturing [22]. They clarified the mechanical performances and electrical resistances of dissimilar and multi-layered Al—Cu sheets, and discussed the feasibility of applying USW to Al—Cu battery cells.

Several other studies have shown that the welding conditions significantly influence bond characteristics between different combinations of dissimilar metals such as Al alloy to steel [23–30], Al alloy to Ti alloy, [31,32] and Al alloy to Mg alloy [33–35]. In general, it is believed that oxide fracture at the mating interface and direct contact between newly formed surfaces can lead to weld formation during ultrasonic welding. These phenomena are thought to be caused by localized deformation in the vicinity of the weld interface [2,5,27,31].

* Corresponding author.
E-mail address: fujii@material.tohoku.ac.jp (H.T. Fujii).

https://doi.org/10.1016/j.matchar.2018.03.010
Received 14 November 2017; Received in revised form 7 March 2018; Accepted 8 March 2018
Available online 08 March 2018
1044-5803/

However, this hypothesis has been accepted without detailed supporting characterization. In particular, there are few systematic studies that reveal the nature of ultrasonic weld formation between Al alloys and Cu. Since high mechanical performance and electrical reliability are the primary requirements of dissimilar welds between these metals, it is essential to provide a scientific basis for weld formation in order to develop ultrasonic Al—Cu welding as a fundamental technology.

The goal of the current work is to improve understanding of the fundamental phenomena involved in weld formation during USW of an Al alloy to Cu. A systematic approach was used to clarify the behavior of the oxide layer, localized deformation in the vicinity of the interface, and formation of intermetallic compound layers via interfacial microstructure characterization.

2. Experimental

This study used sheets of the commercial Al alloy 1050-H24 and Cu sheets with both dimensions of $50 \times 10 \times 1.0\,\text{mm}^3$. Al alloy 1050-H24 samples with 5 μm anodized oxide layers were also used to observe oxide layer behavior near the weld interface during USW. The rolling direction (RD) of the specimens was set perpendicular to the direction of ultrasonic vibration. The specimen coordinate system was defined by the normal direction (ND), vibrating direction (VD), and RD, as shown in Fig. 1. The horn tip was square with 6 mm sides. Thus, the welding area was approximately $6 \times 6\,\text{mm}^2$. The surfaces of the ultrasonic horn and anvil were knurled to prevent them from slipping on the specimens. Table 1 lists the welding parameters used in this study. During USW, the temperature was measured using a type-K thermocouple embedded in the interface between the Al alloy and Cu sheets.

To evaluate the specimen weld strengths, lap shear tensile strength tests were performed at a crosshead speed of 3 mm/min. Although the standard for lap shear strength test is 1 mm/min, we chose 3 mm/min to collect more data by the reduction of testing time. The tensile direction was set perpendicular to the direction of ultrasonic vibration. The microstructures of the welds were characterized using a field emission gun SEM (FEG-SEM). The specimens for microstructural characterization were cut from the welded specimen and mounted in conductive resin. They were ground with SiC abrasive paper in water and then polished with diamond paste. Finally, a surface suitable for microstructural characterization was prepared in a colloidal silica solution on a vibratory polisher. Anodized oxide layers around the weld interface were identified via energy-dispersive X-ray spectroscopy (EDS) performed using the SEM equipment. Electron backscatter diffraction (EBSD) analyses were performed to observe the crystallographic microstructures. The electron beam was scanned using 0.7 μm steps in the vibrating direction-normal direction (VD-ND) plane. In order to understand the behaviors of the interfacial reactions at the weld interface during USW, scanning transmission electron microscopy (STEM) was used to observe specific interfacial areas identified via focused-ion beam (FIB) micro-sampling.

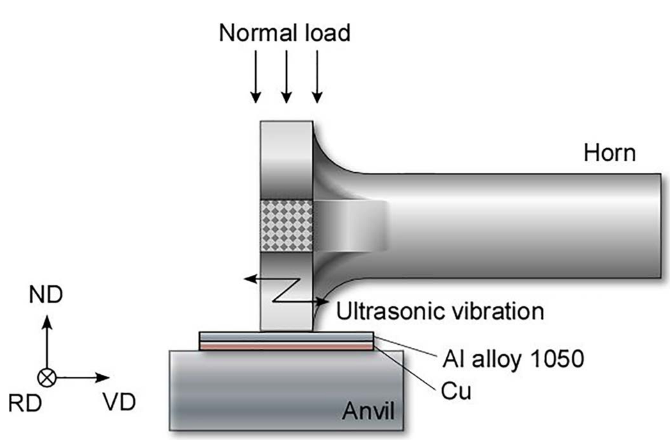

Fig. 1. Schematic of ultrasonic welding, as performed in this study.

Table 1
Ultrasonic welding conditions used in this study.

Material	Thickness, t/mm	Ultrasonic vibration		Normal load, F/N	Welding time, t/s
		Frequency, F/kHz	Amplitude, A/μm		
A1050-H24	1.0	19.15	51	589	0.10–0.50
Cu	1.0				

3. Results and Discussion

3.1. Behavior of the Aluminum Oxide Layer at the Weld Interface

It is essential to clarify the behavior of the natural aluminum oxide film at the weld interface in order to understand weld formation during USW of Al to Cu. However, it is difficult to identify the natural aluminum oxide film near the ultrasonic weld between Al and Cu because it is less than a few nanometers thick [36] and is expected to be broken at the weld interface after USW. Therefore, we performed USW of the anodized Al 1050 to Cu and then observed the post-weld anodic aluminum oxide layer with the intent of deriving the behavior of the natural aluminum oxide film during USW. To confirm that the behavior of anodic aluminum oxide layer during USW was similar to that of the natural aluminum oxide film, the thermal and mechanical behaviors of the USWs of anodized and non-anodized Al 1050 to Cu were compared.

Thermal hysteresis was measured to aid in understanding heating during USW. Fig. 2 shows (a) a typical thermal profile measured using a thermocouple embedded between the Al alloy and Cu sheets prior to USW and (b) the relationship between the peak temperature and welding time in the ultrasonically welded anodized and non-anodized Al/Cu specimens. Thermal profiles show that the USW heating time is approximately 0.50–2.0 s, and that the peak temperature increases to approximately 350 K–600 K. The peak temperature exceeds the recrystallization temperature (0.4 times the melting point) when the welding time is over 0.30 s, regardless of whether an anodic aluminum oxide layer is present at the weld interface. As can be seen in Fig. 2(b), peak temperatures are slightly higher during USW of anodized Al than during USW of Al. According to Yang et al. [14], the hard inclusions at the ultrasonic weld interface lead to larger stresses, causing more extensive matrix material plastic deformation near the inclusions than at regions away from them. In the case of USW of anodized Al to Cu, the anodic aluminum oxide layer at the weld interface acts as a stress riser. As a result, slightly more deformation heating occurs during USW of anodized Al than during USW of Al.

Fig. 3 shows the dependence of the lap shear strength on the welding time of the non-anodized and anodized Al alloy/Cu specimens. The specimens were not welded when a welding time of < 0.10 s was used. The lap shear strength increased with the welding time up to 0.40 s, regardless of whether an anodic aluminum oxide layer was present at the weld interface. Fig. 3(b) shows examples of typical tensile-tested coupon fracture surfaces with two different fracture modes. The fracture mode changes from interfacial debonding to base material fracture when the welding time exceeds 0.35 s and 0.40 s during USW of Al alloy and anodized Al, respectively. In the specimens fractured at the base material, there was a reduction in lap shear strength at the welding time longer than 0.4 s. This would be attributed to the softening of Al alloy caused by the heating and the decrease in thickness of the weld region during USW. The lap shear strengths of the anodized Al-based specimens are slightly smaller than those of the Al-based specimens at all welding times. This is because the residual anodic aluminum oxide layer at the weld interface reduces the directly welded Al/Cu area. However, the specimens made from anodized Al and Cu